Y. Lin, W.-C. Li, Z. Ren, and C. T.-C. Nguyen, "A resonance dynamical approach to faster, more reliable micromechanical switches," *Proceedings*, 2008 IEEE Int. Frequency Control Symp., Honolulu, Hawaii, May 19-21, 2008, pp. 640-645.

A Resonance Dynamical Approach to Faster, More Reliable Micromechanical Switches

Yang Lin, Wei-Chang Li, Zeying Ren, and Clark T.-C. Nguyen
Department of Electrical Engineering and Computer Science
University of California at Berkeley
Berkeley, CA 94720 USA

***Abstract*—The resonance and nonlinear dynamical properties of micromechanical structures have been harnessed to demonstrate an impacting micromechanical switch with substantially higher switching speed, better reliability (even under *hot switching*), and lower actuation voltage, all by substantial factors, over conventional RF MEMS switches. The particular resoswitch implementation demonstrated in this work comprises a wine-glass mode disk resonator, driven hard via a 2.5V amplitude ac voltage at its 61-MHz resonance frequency so that it impacts electrodes along an orthogonal switch axis, thereby closing a switch connecting a signal through switch axis electrodes. The 61-MHz operating frequency corresponds to a switching period of 16ns with an effective rise time of ~4ns, which is more than 50 times faster than the μs-range switching speeds of the fastest conventional (non-resonant) RF MEMS switches. Furthermore, with the signal on during switching, a capacitive version of the switch has *hot switched* for more than 16.5 *trillion* cycles without failure, which is substantially more than the 100 billion cycles normally posted by conventional RF MEMS switches. The reliability of the present resoswitch benefits from the high stiffness of its actuating disk resonator, which provides a large restoring force with which to overcome sticking forces; and from the energy stored via resonance vibration that provides a momentum that further increases the effective restoring force. Resonance operation in turn allows the actuation voltage amplitude to be a mere 2.5V, despite the large spring restoring force. Such mechanically resonant switches (dubbed "resoswitches") used in place of the switching transistors in switched-mode power converters and power amplifiers stand to greatly enhance efficiencies by allowing the use of much higher power supply voltages than allowable by transistors.**

***Index Terms*—microelectromechanical devices, microresonator, nonlinear resonance dynamics, RF MEMS, switch, power amplifier, power converter.**

I. Introduction

RF MEMS switches operating at RF to millimeter-wave frequencies substantially outperform p-i-n diode and field-effect transistor (FET) counterparts in insertion loss, isolation, and switch figure of merit (*FOM*) [1][2]. Unfortunately, their much slower switching speeds (e.g., 1-15 μs versus the 0.16-1ns [3] of FET's) and cycle lifetimes on the order of 100 billion cycles (for the good ones) relegates them mainly to antenna switching, reconfigurable aperture, and instrumentation applications, and precludes them from much higher volume applications, such as switched-mode power amplifiers and power converters.

Indeed, the benefits afforded to switched-mode power applications that would ensue if the transistors they presently employ were replaced by switches with *FOM*'s on the order of those exhibited by RF MEMS switches would be enormous. For example, switched-mode power amplifiers that ideally should be able to achieve 100% drain efficiency presently cannot attain such values in practical implementations, in part because the transistors they use for switching exhibit large input capacitors (for small "on" resistances) and are often limited in the supply voltages they can support. On the other hand, MEMS switches, being made of metal, have very small "on" resistances and would be able to support higher supply voltages. However, if they are to be used in switched-mode power applications, their actuation voltages would need to be lowered substantially (from >50V down to the single-digit volt range), their speeds would need to be much higher (e.g., ns switching times), and their reliability enhanced substantially, since typical power amplifier and converter applications would require cycle counts in the quadrillions.

Pursuant to achieving a switch suitable for power amplifier and converter applications, this work demonstrates a micromechanical switch, dubbed the "resoswitch" [4], that harnesses the resonance and nonlinear dynamical properties of its mechanical structure to greatly increase switching speed and cycle count (even under hot switching), and lower the needed actuation voltage, all by substantial factors over existing RF MEMS switches. The device comprises a wine-glass mode disk resonator driven hard via a 2.5V amplitude ac voltage at its 61-MHz resonance frequency so that it impacts electrodes along an orthogonal switch axis, thereby closing a switch connecting a 10V source to the switch electrode. The 61-MHz operating frequency corresponds to a switching period of 16ns with an effective rise time of <4ns, which is more than 200 times faster than the μs-range switching speeds of the fastest RF MEMS switches. Furthermore, since the voltage source is on during switching, the switch essentially *hot switches* with a demonstrated lifetime exceeding 16.5 *trillion* cycles without failure, but with some observable degradation.

II. Basic Resoswitch Operation and Advantages

The advantages provided by a switch that harnesses resonance dynamics are perhaps best conveyed via comparison with conventional RF MEMS switch counterparts that do not. For this purpose, Fig. 1 presents the top view and cross-section of a typical conventional RF MEMS switch, in this case one demonstrated by Goldsmith [1]. As shown, this switch consists of a metal membrane (or beam) suspended above a switch contact electrode that can be electrostatically pulled down onto the contact electrode by applying a sufficient actuation voltage V_{switch} to an underlying "gate" electrode. For the case of a sus-

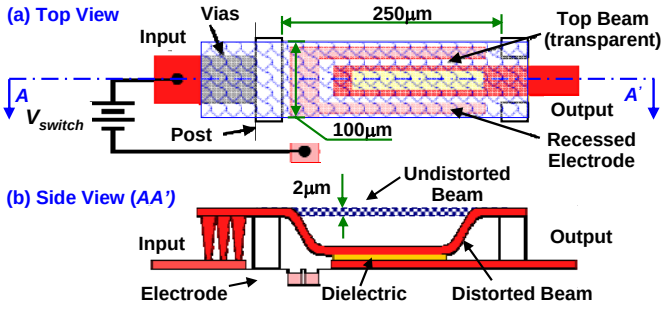

Fig. 1: Schematic of a conventional micromechanical switch showing both (a) top and (b) cross-sectional side views, and indicating key dimensions.

pended beam with the typical dimensions indicated in Fig. 1, and with a beam-to-electrode gap spacing of 2 μm, the effective stiffness of the beam (at its midpoint) is on the order of 57 N/m, and the required actuation voltage is about 55V. This voltage can be lowered by either reducing the beam stiffness or reducing the gap spacing between the beam and the underlying electrode. Both of these approaches, however, come with drawbacks: the former reduces the restoring force with which the beam can overcome stiction forces, thereby sacrificing its reliability; while the latter increases the capacitance of the switch, thereby reducing its off-state isolation (and its *FOM*). It is these trade-offs that constrain the actuation voltages of RF MEMS switches to the 50V range, which in turn constrains their stiffnesses and masses to values that limit switching speeds to microseconds and that compromise reliability.

Suppose now that the application for the switch is one that requires periodic switching, where the switch must turn on and off in with nearly constant period. Some of the highest volume applications of switches, namely switched-mode power converters [5]-[8] and power amplifiers [9][10], in fact operate in such a mode, where their switches switch continuously with essentially constant period within specified bandwidths. The use of a micromechanical switch in place of the switching transistor in these applications stands to greatly enhance performance by raising the *FOM* of the switch and by allowing the use of much higher supply voltages (e.g., 10V vs. the 1V limit of conventional CMOS) [11], which raises the efficiency of switched-mode power amplifiers and raises the voltage levels achievable by boosting power converters.

Although it might be possible to utilize a properly scaled (to nanodimensions [12]) non-resonant switch that switches with constant period for such applications, it is much more advantageous to employ the resonance characteristics of the mechanical structure. In particular, if the switch of Fig. 1 were driven by an actuation voltage at the resonance frequency of the beam, then the actuation voltage V_{switch} required to attain the same displacement of the beam (i.e., to close the switch) would be Q times smaller than that for off-resonance actuation inputs. In other words, if the beam had a Q of 5,000, then the needed actuation voltage would shrink from 55V, to only 11mV. In addition, the resonance frequency of a mechanical structure is close to the highest frequency at which it can operate, so operation at resonance maximizes the switching speed.

Orders of magnitude lower actuation voltage and faster switching speed already constitute tremendous improvements, but the advantages of resonance operation do not stop, here. In particular, the actuation voltage (from the above example) need not be as small as 11mV; rather, reduction of the actuation voltage down to 1V would already be compatible with advanced CMOS transistor technologies. To back off the actuation voltage, a designer might either raise the stiffness of the beam, by making it thicker or by shrinking its length dimension; or reduce the beam-to-drive electrode overlap capacitance, by increasing the beam-to-drive electrode gap spacing or by reducing its overlap area.

Raising stiffness is quite beneficial, since it effectively raises the speed of the switch by increasing its resonance frequency. It also improves the reliability of the switch by increasing the restoring force available to overcome adhesion forces that might otherwise cause the beam to stick to the electrode. For example, if the thickness of the beam of Fig. 1 were increased to 5 μm, and its length reduced to 150 μm, then the effective beam stiffness at its midpoint would become 4,150 N/m, raising its frequency range (i.e., its resonance frequency) from 180 kHz to 1.06 MHz, which corresponds to a switching speed of $[(4)(1.06)(10^6)]^{-1}$ = 236 ns, where switching speed here is approximated as one-fourth the switching period. The available restoring force is also increased by this design change from 0.11 mN to 8.3 mN, as illustrated by the following calculation:

$$F_{restore} = kd = \begin{cases} 0.11\,\text{mN} \Leftarrow k = 57\ \text{N/m} \\ 8.3\,\text{mN} \Leftarrow k = 4{,}150\ \text{N/m} \end{cases} \quad (1)$$

where $F_{restore}$ is the restoring force, k is the stiffness of the beam, and d (=2 μm) is the distance between the beam and the contact electrode. Finally, despite the increase in stiffness, the needed resonance actuation voltage amplitude remains quite small, at a calculated 94 mV.

Beyond increasing stiffness, the other option for backing off on actuation voltage, i.e., decreasing the beam-to-electrode overlap capacitance, is also quite beneficial, since it reduces the off-state capacitance of the switch, thereby raising its *FOM*. Thus, the use of resonance operation improves switch performance in both the mechanical and electrical domains.

As will be seen, the nonlinear dynamical behavior of the resoswitch offers even greater advantages for specific switched-mode applications, such as bandwidth and duty cycle control, which are important for power amplifiers and power converter applications, respectively.

III. Wine-Glass Disk Resoswitch

Although the resoswitch example so far discussed does present clear advantages over its non-resonant counterpart, its use of a clamped-clamped beam structure confines it to resonance frequencies lower than about 100 MHz, since anchor losses plague this design at higher frequencies [13]. To attain the GHz frequencies demanded by switched-mode power amplifier applications, disk [14] or ring [15] resonator geometries are much more appropriate.

With this in mind, Fig. 2 presents schematics describing the structure and operation of one simple rendition of a resoswitch that comprises a capacitively-transduced wine-glass disk micromechanical resonator [16] (c.f., Fig. 3) made in a conductive material (preferably, a metal) and surrounded by four electrodes, two of which are situated along an indicated input axis having larger electrode-to-resonator gaps than their counterparts along an orthogonal switch axis. To operate the

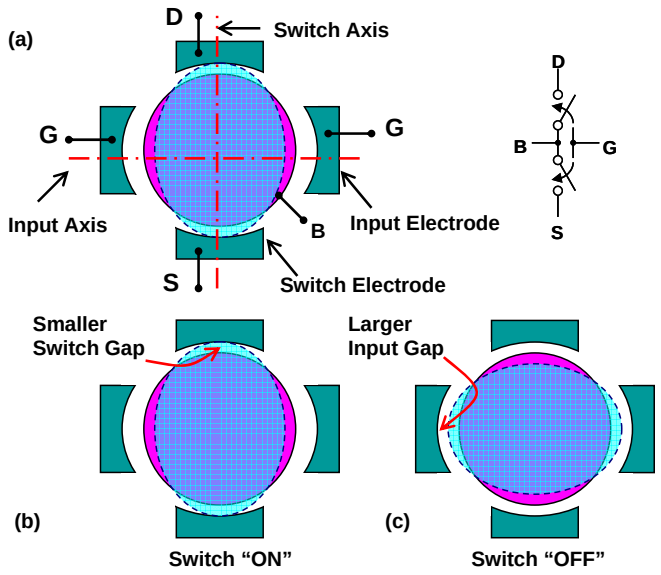

Fig. 2: Schematics showing (a) the physical structure of the micromechanical resoswitch, identifying its ports and equating it to a functional equivalent circuit; (b) its "on"; and (c) its "off" states.

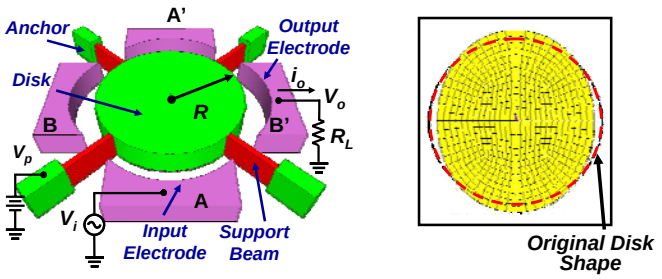

Fig. 3: (a) Perspective-view schematic of a micromechanical wine-glass-mode disk resonator in a typical two-port bias and excitation configuration (where A,A' are electrically connected, as are B,B'). (b) ANSYS simulated wine-glass mode shape.

switch, an ac input voltage at the wine-glass mode disk resonance frequency is applied to the input electrodes (along the input axis), electrically forcing the disk into the wine-glass mode shape delineated by the dotted curve in Fig. 2(a). As the resonance amplitude rises, the disk eventually impacts the (closer) electrodes along the switch axis, as shown in Fig. 2(b). This then ideally steals energy from the disk, effectively limiting its amplitude so that when the disk elongates along the input axis on the next cycle, it does not impact the (more distant) input electrodes, as shown in Fig. 2(c). Essentially, in this structure, control electrodes more distant from the disk are used to drive the disk into its resonance mode shape (indicated by the dotted curve), where at sufficient amplitude it impacts closer electrodes along the orthogonal axis, closing the switch at a frequency equal to the resonance frequency of the disk. Because the input is applied at the resonance frequency of the disk, the required input voltage amplitude that effects switching along the switch axis is quite small, on the order of 1-3V, which is much smaller than the >50V required by most conventional RF MEMS switches.

As already mentioned, for the switched-mode power amplifier and power converter application targets of this work, the cycle count of the resoswitch would need to be much larger (3 quadrillion) than so far achieved by conventional non-resonant RF MEMS switches (1 trillion). In this regard, the

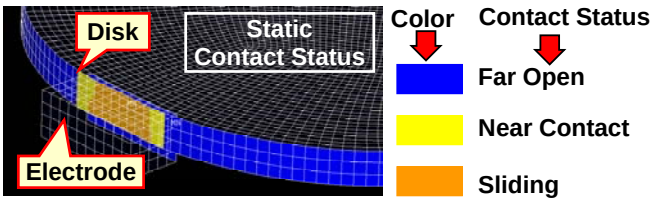

Fig. 4: Finite element simulation of the disk impacting the electrode with color map showing the degree of contact over different regions of the disk-to-electrode interface.

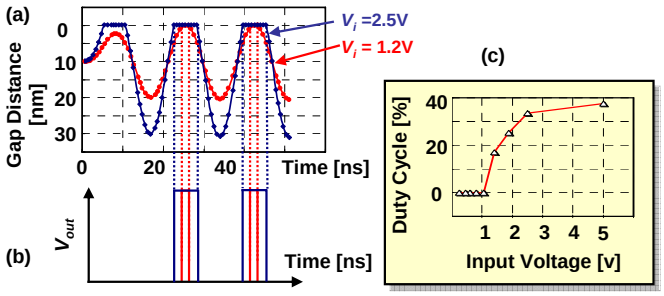

Fig. 5: ANSYS simulated (a) gap spacing and (b) resulting output voltage waveforms versus time for different actuation voltages. (c) Plot of duty cycle versus input voltage generated from several (a),(b)-type simulations.

reliability of the present resoswitch benefits from two major advantages: 1) the stiffness of its actuating disk resonator is on the order of 1.15×10^6N/m (for a 61-MHz wine-glass disk), which is several orders larger than that of a conventional RF MEMS switch, so provides a substantially larger restoring force with which to overcome sticking forces; and 2) the energy stored via resonance vibration of the device provides a momentum that further increases the effective restoring force and that reduces in some cases the force with which the disk edge impacts the switch electrode. Again, the use of such a large spring restoring force is made possible by resonance operation, under which the displacement of the actuator is *Q* times larger than off-resonance, allowing a mere 1-3V amplitude drive voltage to generate impacting switch axis amplitudes in spite of the large stiffness of the disk structure.

Fig. 4 presents a finite element simulated (using ANSYS) topographical plot showing the sliding distribution seen at the disk edge-to-switch axis electrode interface upon impact. From multiple such simulations, plots of gap spacing versus time can be generated, two of which are shown in Fig. 5(a) for cases where 1.25V and 2.5V input signal voltages are applied. Here, the larger 2.5V input clearly generates the larger disk vibration amplitude, and as shown, the longer resulting impact interval. Fig. 5(b) shows the voltage waveforms generated by switch contacting, clearly showing that the duty cycle of the output waveform is controlled by how hard the resoswitch is driven. In particular, when the resoswitch is driven softly, so that it only barely touches the switch axis electrodes, the duty cycle is very small. When driven very hard, the duty cycle rises closer to its 50% maximum. Fig. 5(c) plots duty cycle versus input voltage (using FEA-simulated points) to more clearly illustrate the relationship between input amplitude and output duty cycle. Such control of duty cycle is very useful for switched-mode power converters, for which the conversion ratio is often set by duty cycle.

Not only is the duty cycle adjustable, but so is the bandwidth of the resoswitch. In particular, as shown in Fig. 6, the bandwidth over which impacting occurs can also be controlled

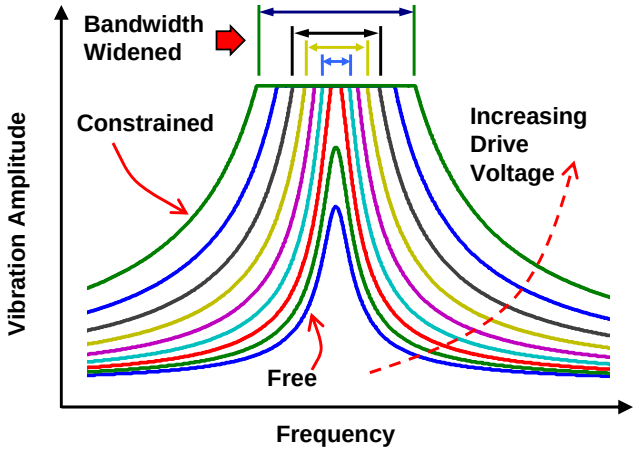

Fig. 6: Expected frequency response illustrating bandwidth widening via nonlinear impact limiting.

by the amplitude of the ac input voltage. In effect, the larger the input voltage amplitude, the lower the frequency of first limiting on the frequency characteristic of the device, and the higher the frequency of last limiting. This bandwidth-widening is a nonlinear dynamical effect that provides simultaneous high-*Q* and wide bandwidth—something not generally available in purely linear systems, where high *Q* often means small bandwidth. In particular, nonlinear resonance dynamics provides on the one hand high *Q* along the input axis, which lowers the required input ac voltage; while also providing on the other hand a wide effective bandwidth along the switch (or output) axis. The availability of simultaneous high-*Q* and wide bandwidth obviously benefits transmit power amplifier applications in communications, since it permits wide frequency modulations on the transmitted signal while simultaneously lowering the input capacitance needed to operate the device with a given input signal amplitude.

IV. Experimental Results

To demonstrate the resoswitch, doped polysilicon wineglass mode disk resonators based on the design and fabrication process of [16] were employed. Fig. 7(a) presents the SEM of one of the 61-MHz wineglass disk resonators used in this work, with a zoom-in shot in (b) showing the tiny gap between the disk and its switch electrode. For most power amplifier and converter applications, the resoswitch should be constructed of metal, not polysilicon, to reduce its contact and series resistance. The use of doped polysilicon in this work does compromise resoswitch performance, especially with regards to the switch "on" resistance, which is dominated by the 1.1 kΩ parasitic resistance R_p of its polysilicon leads and interconnects. Nevertheless, it still allows demonstration of practically all other important resoswitch performance parameters. It should be noted that, despite its high series resistance, the polysilicon version of the resoswitch is actually still quite applicable for use in low current drain switched-mode on-chip dc-to-dc power converters (i.e., charge pumps), such as needed to supply the large dc-bias voltages often required by vibrating resonators and RF MEMS devices [1][13]-[16].

For simplicity in this early demonstration, the strategy of using different electrode-to-disk spacings along the input and switch axes shown in Fig. 2 was not used in this implementation. Rather, the electrode-to-resonator gap spacings for both axes were 100 nm for direct contact switches, in which the conductive disk and electrode materials actually make electrical contact; and about 97 nm for capacitive switches, in which a thin layer of oxide exists over conductive surfaces that prevents electrical contact, but still allows switching through the large capacitance that results when the disk impacts its switch electrodes. For the direct contact version of the resoswitch, one obvious consequence of the use of identical input and switch axis electrode-to-resonator gaps is that the input gets shorted to the disk during operation, which then complicates use of the resoswitch in actual applications. (For example, the Class E power amplifier topology later shown in Fig. 12(b) would not be permissible under these conditions.)

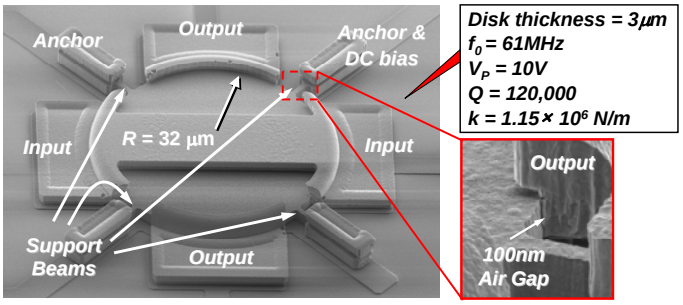

Fig. 7: (a) SEM of the polysilicon resoswitch demonstration vehicle used in this work, which essentially comprises a wine-glass disk resonator with properly spaced and positioned electrodes; and (b) zoom-in on the electrode-to-resonator gap of the device along the switch axis.

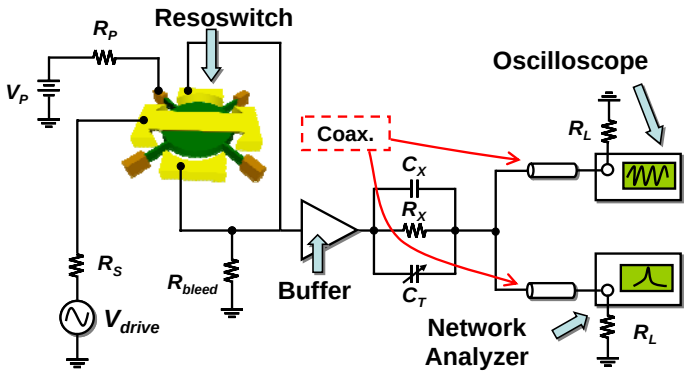

Fig. 8: Test set-up used to evaluate the micromechanical resoswitch.

To deal with input shorting, the test set-up used to measure resoswitch performance, depicted in Fig. 8, uses a less practical configuration, but one still valid for evaluation of switch performance. Here, a dc-bias voltage V_P is applied to the disk structure that is effectively applied to the output node when the switch closes (i.e., comes "on") in the fashion shown in Fig. 2. As shown, this circuit allows both time domain (i.e., oscilloscope) and frequency domain (i.e., network analyzer) observation of the resoswitch output. The output buffer used in this circuit effectively removes the 80pF of coaxial capacitance that would otherwise load the output node of the resoswitch and greatly reduce the signal level due to 3dB bandwidth roll-off. The output buffer, however, is not perfect, as it still loads the output node of the resoswitch with about 4pF. This is large enough to round out the corners of the expected output square wave (c.f., Fig. 5(b)) so that it looks more sinusoidal.

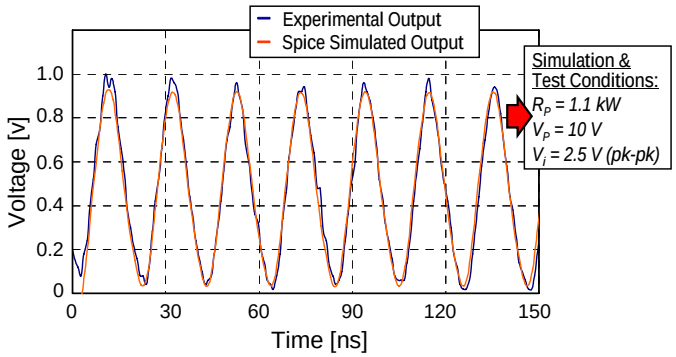

Fig. 9: Oscilloscope (i.e., time domain) waveform and SPICE simulated prediction seen at the resoswitch output node of Fig. 8 when driven by a resonance input signal with 2.5V amplitude.

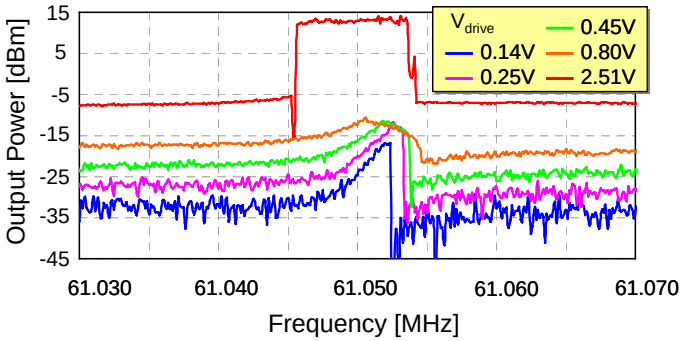

Fig. 10: Frequency response (in vacuum) as measured by a network analyzer of the direct contact version of the resoswitch for varying resonance input ac voltage amplitudes.

Fig. 9 and Fig. 10 present the oscilloscope waveform and swept frequency response spectrum (for various input amplitudes), respectively, of the direct contact resoswitch, verifying switching operation, impact limiting, and also the bandwidth-widening effect previously discussed. Switching clearly occurs when the frequency response grows suddenly and limits with a "flat top", as shown on Fig. 10. This occurs when the voltage amplitude reaches 2.5V. The measured output signal in Fig. 9 has a peak-to-peak amplitude of about 1V, which is the value expected when considering attenuation via the finite 3dB bandwidth of the measurement circuit of Fig. 8, and when considering the voltage divider formed by the parasitic polysilicon interconnect resistance R_p and the bleed resistor R_{bleed}. The signal is not quite a square wave due to bandwidth limitations of the measurement circuit, but the amplitude is correct. To emphasize this point, Fig. 8 also includes a SPICE simulated waveform that includes the effects of 1.1 kΩ of parasitic resistance R_p and 3.5 pF of buffer input capacitance, and that clearly matches the measured waveform.

Fig. 11 presents a measured plot of output power (seen at the switch axis output node) versus frequency. Here, the buffer of Fig. 8 was not used, so load-induced attenuation somewhat compromised the measurement, resulting in a measured output power considerably lower than in Fig. 10. Nevertheless, Fig. 11 does verify the nonlinear resonance dynamical behavior of the resoswitch, since the bandwidth does indeed widen as the input voltage amplitude increases.

To evaluate reliability, the resoswitch was operated continuously with V_P = 10V for 75 hours (~3 days or 16.5 trillion cycles) without failure at a frequency of 61 MHz [4], which is a frequency in the flat region of Fig. 10, and thus, a frequency where impacting occurs. Although no failure was observed,

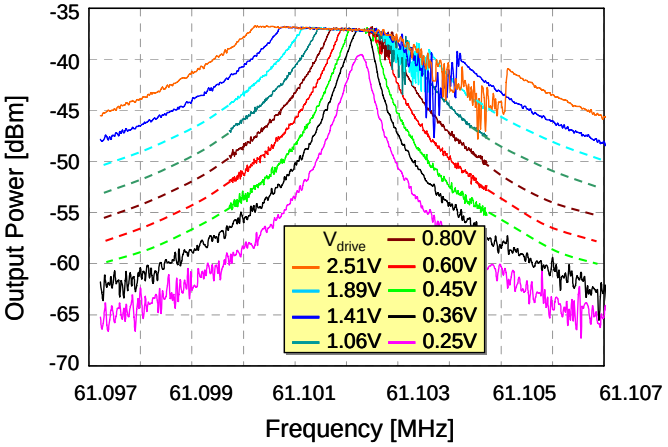

Fig. 11: Measured output signal power versus frequency for the capacitive version of the resoswitch. Here, the output power clearly limits when the disk impacts the switch electrode.

degradation was seen, where after about 1.5 days, the output voltage began to decrease significantly. Although 1.5 days corresponds to 7.7 trillion cycles at 61 MHz, which is more than two orders of magnitude higher than the 100 billion cycles typically achieved by (good) RF MEMS switches, there is still cause for concern, here, since typical switched-mode power applications will require quadrillions of cycles. More study into the degradation mechanism is needed, but one possible reason for the observed degradation could be the growth of a thicker oxide or other dielectric on the switch contact interfaces. In the future, resoswitches constructed of metal with engineered contact surfaces will be investigated.

V. Conclusions

In this work, the resonance and nonlinear dynamical properties of a micromechanical wine-glass disk have been harnessed to demonstrate an impacting micromechanical switch with substantially higher switching speed, better reliability (even under hot switching), and lower actuation voltage, all by substantial factors, over existing RF MEMS switches. Although next generation versions of this resoswitch constructed in metal material [22] should be more widely applicable, the present polysilicon version can still find application to low current drain applications, such as Dickson charge pumps [5], where replacement of diodes with resoswitches should allow a very high output voltage, suitable for dc-biasing of capacitively transduced micromechanical resonators.

Perhaps the best way to gauge the benefits of the described resoswitch is by comparison with other switches. To this end, Table I compares the described micromechanical resoswitch with transistor FET and RF MEMS switch counterparts, showing clear advantages in maximum supply voltage and input capacitance over transistor FET's, and in actuation voltage and speed over RF MEMS switches. The *'ed items also convey expectations that a metal version of the resoswitch should be able to match the series resistance and *FOM* of a conventional RF MEMS switch.

Although the device-to-device comparisons are already favorable for the resoswitch, the advantages provided by the resoswitch are perhaps best elucidated in the context of an application. To this end, Fig. 12 shows the circuit topologies of (a) a conventional Class E power amplifier (PA) using a transistor switch device; and (b) one simplified rendition of the

TABLE I. ON-CHIP SWITCH COMPARISON

Parameter	FET	RF MEMS	Resoswitch
Actuation Voltage	1-3 V	20-80 V	2.5 V
Off State Power	0.2-3μW	0	0
Switching Time	0.16-1 ns [3]	1-300 μs	~ 4 ns
Life Time	Very Long	100 Billion [19]	> 16.5 Trillion
On Resistance	0.5 Ω [17]	0.1-1 Ω [20]	0.1-1 Ω*
Input Capacitance	20 pF [17]	1-10 fF [21]	20-30 fF
$FOM = 1/(2\pi R_{on}C_{off})$	590 GHz [18]	63 THz	>30 THz*

* Potentially achievable by a metal version.

same amplifier utilizing the vibrating micromechanical resonant switch demonstrated in this work. The use of a micromechanical resoswitch in place of the switching transistor in this application stands to enhance performance as follows:

1) It allows the use of much higher voltages (e.g., 10V vs. the 1-3V limit of conventional CMOS) [11]. This then allows the resoswitch rendition to directly drive the 50Ω load, and thereby dispense with the lossy matching network needed by the transistor version. Removal of the matching network and raising the driven impedance from 2Ω to 50Ω can raise the efficiency of a Class E power amplifier by as much as 23%.

2) The use of the resoswitch further allows the same or smaller "on" resistance than its FET counterpart, but with substantially smaller input capacitance, e.g., only 20fF for the resoswitch versus 20pF for a CMOS PA switch—a 1000× difference that removes much of the input power that would otherwise be needed to drive the PA. Again, better efficiency ensues.

Again, the above benefits ensue only when the resoswitch is implemented in a metal structural material. Work towards this is in progress.

Acknowledgment: This work was supported by DARPA.

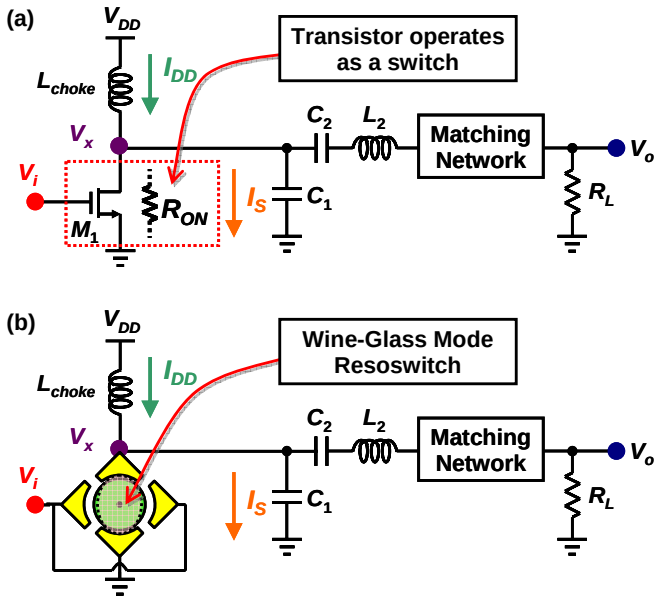

Fig. 12: Circuit topologies of (a) a conventional Class E amplifier using a transistor switch device; and (b) one simplified rendition of the proposed Class E amplifier utilizing the described vibrating micromechanical resonator switch.

REFERENCES

[1] Z. J. Yao, S. Chen, S. Eshelman, D. Denniston, and C. Goldsmith, "Micromachined low-loss microwave switches," *IEEE/ASME J. Microelectromech. Syst.*, vol. 8, no. 2, pp. 129-134, June 1999.

[2] P. D. Grant, *et al.*, "A comparison between RF MEMS switches and semiconductor switches," *Proceedings*, ICMENS, Aug. 25-27, 2004, pp. 515-521.

[3] H. Kamitsuna, *et al.*, "A fast low-power 4×4 switch IC using InP HEMTs for 10-Gbit/s Systems," *Proceedings*, IEEE CSIC, Jul. 2004, pp. 97–100.

[4] Y. Lin, W.-C. Li, Z. Ren, C. T.-C. Nguyen, "The micromechanical resonant switch ("Resoswitch")", *Tech. Digest*, 2008 Solid-State Sensor, Actuator, and Microsystems Workshop, Hilton Head, South Carolina, June 1-5, 2008, pp. 40-43.

[5] Mohan, Ned, Undeland, *et al.*, *Power Electronics: Converters, Applications and Design*. Hoboken, NJ: John Wiley & Sons, 2003.

[6] J. F. Dickson, "On-chip high-voltage generation in MNOS integrated circuits using an improved voltage multiplier technique," *IEEE J. Solid-State Circuits*, vol. 11, no.3, pp.374-378, June 1976.

[7] R. D. Middlebrook, "Small-signal modeling of pulse-width modulated switching-mode power converters," *Proc. EEE*, vol. 76, no. 4, pp.343-354, Apr. 1988.

[8] S. Rajapandian, *et al.*, "High-voltage power delivery through charge recycling," *IEEE J. Solid-State Circuits*, vol. 41, no 6, Jun. 2006, pp.1400-1410.

[9] N.O. Sokal, *et al.*, "Class E-A new class of high-efficiency tuned single-ended switching power amplifiers," *IEEE J. Solid-State Circuits*, vol. 10, no. 3, pp.168–176, June 1975.

[10] K.-C. Tsai, Gray, P.R., "A 1.9GHz 1W CMOS class-E power amplifier for wireless communications," *IEEE J. Solid-State Circuits*, vol. 34, no. 7, pp. 962-970, Jul. 1999.

[11] S. Wolf, *Silicon processing for the VLSI era volume 3 - The submicron MOSFET*. Sunset Beach, CA: Lattice Press, 1995.

[12] W.Y. Choi, H. Kam, D. Lee, J. Lai, Tsu-Jae King Liu, "Compact Nano-Electro-Mechanical Non-Volatile Memory (NEMory) for 3D Integration", *Technical Digest*, IEEE Int. Electron Devices Mtg., Washington, DC, Dec. 2007, pp.603-606.

[13] K. Wang, A.-C. Wong, and C. T.-C. Nguyen, "VHF free-free beam high-*Q* micromechanical resonators," *IEEE/ASME J. Microelectromech. Syst.*, vol. 9, no. 3, pp. 347-360, Sept. 2000.

[14] J. Wang, Z. Ren, and C. T.-C. Nguyen, "1.156-GHz self-aligned vibrating micromechanical disk resonator," *IEEE Trans. Ultrason., Ferroelect., Freq. Contr.*, vol. 51, no. 12, pp. 1607-1628, Dec. 2004.

[15] Y. Xie, S.-S. Li, Y.-W. Lin, Z. Ren, and C. T.-C. Nguyen, "1.52-GHz μmechanical extensional wine-glass mode ring …," *IEEE Trans. Ultrason., Ferroelect., Freq. Contr.*, vol. 55, no. 4, pp. 890-907, April 2008.

[16] Y.-W. Lin, S. Lee, S.-S. Li, Y. Xie, Z. Ren, C. T.-C. Nguyen, "Series-resonant VHF micromechanical resonator reference oscillators," *IEEE J. Solid-State Circuits*, vol. 39, no. 12, pp. 2477-2491, Dec. 2004.

[17] Agilent Technologies, "Agilent solid state switches: selecting the right switch technology for your application," 2007.

[18] D.A. Blackwell, *et al.*, "X-band MMIC switch with 70dB isolation and 0.5 dB insertion loss," *Digest of Papers*, IEEE Microwave and Millimeter-Wave Monolithic Circuits Symposium, May 12-16, 1995, pp 97-100.

[19] S. Majumder, *et al.*, "A packaged, high-lifetime ohmic MEMS RF switch," *Microwave Sym. Dig.*, IEEE MTT-S, vol.3, pp. 1935-1938, June 8-13, 2003.

[20] J. B. Muldavin, *et al.*, "High-isolation inductively-tuned X-band MEMS shunt switches," *Microwave Sym. Dig.*, IEEE MTT-S, vol.1, pp. 169-172, June 11-16, 2000.

[21] G. M. Rebeiz, et al., "RF MEMS Switches and switch circuits," *IEEE Microwave Magazine*, Dec. 2001, pp. 59-71.

[22] W.-L. Huang, *et al.*, "Fully monolithic CMOS nickel micromechanical resonator oscillator," *Tech. Dig.*, 2008 IEEE MEMS Conf., pp. 10-13.